Electronic Supplementary Information

Perylenetetracarboxy-3,4:9,10-diimide derivatives with large two-photon absorption activity

Eleonora Garoni, Filippo Nisic, Alessia Colombo, Simona Fantacci, Gianmarco Griffini, Kenji Kamada, Dominique Roberto, Claudia Dragonetti

TPA details

Table S1. TPA cross-section values and errors (in parentheses) in unit of GM obtained by changing the incident power (power-scan)

λ (nm)	P1	P2	P3	P4
720	770 (60)	1530 (120)	1060 (120)	630 (50)
680	510 (40)	1810 (150)	900 (70)	450 (40)
639	1280 (100)	3340 (270)	2390 (200)	1000 (80)

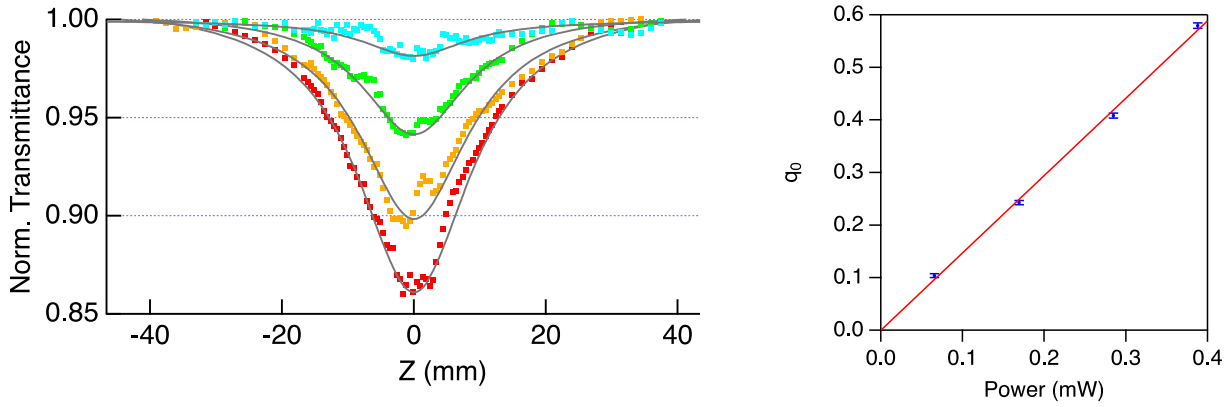

Figure S1. Open aperture Z-scan traces (dots) of **P1** in dichloromethane (1.1 mM, pathlength = 2 mm) at various incident powers (0.07–0.38 mW) at 638 nm with the theoretical fitting curves (solid line) with TPA for temporal and spatial Gaussian pulses (left) and the plot of the obtained on-axis peak two-photon absorbance q_0 with error bars ($\pm\sigma$) against the incident powers with a liner fit (right).

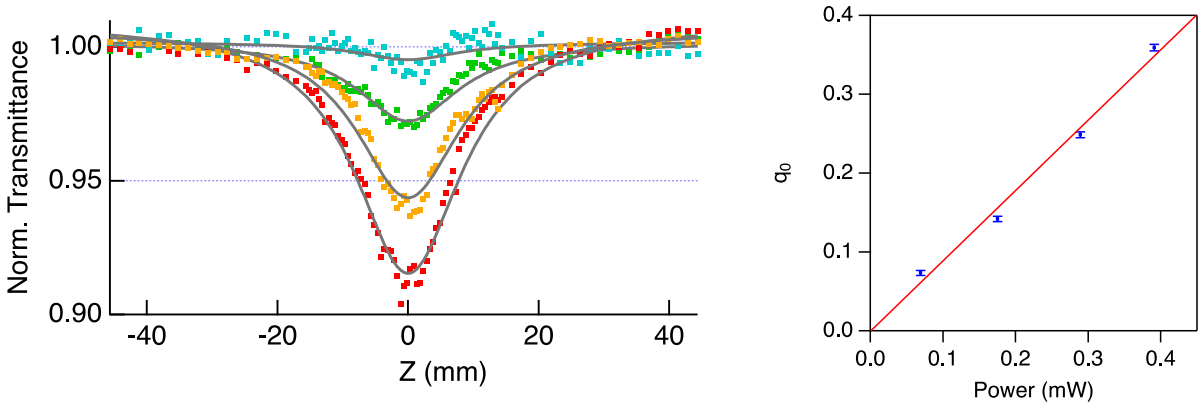

Figure S2. Open aperture Z-scan traces (dots) of **P2** in dichloromethane (0.33 mM, pathlength = 2 mm) at various incident powers (0.07–0.39 mW) at 638 nm with the theoretical fitting curves (solid line) with TPA for temporal and spatial Gaussian pulses (left) and the plot of the obtained on-axis peak two-photon absorbance q_0 with error bars ($\pm\sigma$) against the incident powers with a liner fit (right).

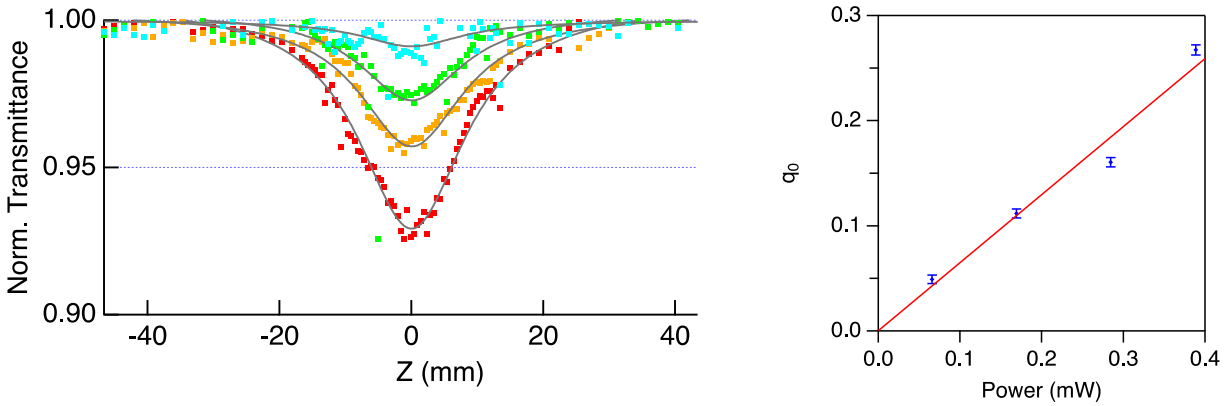

Figure S3. Open aperture Z-scan traces (dots) of **P3** in dichloromethane (0.32 mM, pathlength = 2 mm) at various incident powers (0.07–0.39 mW) at 638 nm with the theoretical fitting curves (solid line) with TPA for temporal and spatial Gaussian pulses (left) and the plot of the obtained on-axis peak two-photon absorbance q_0 with error bars ($\pm\sigma$) against the incident powers with a liner fit (right).

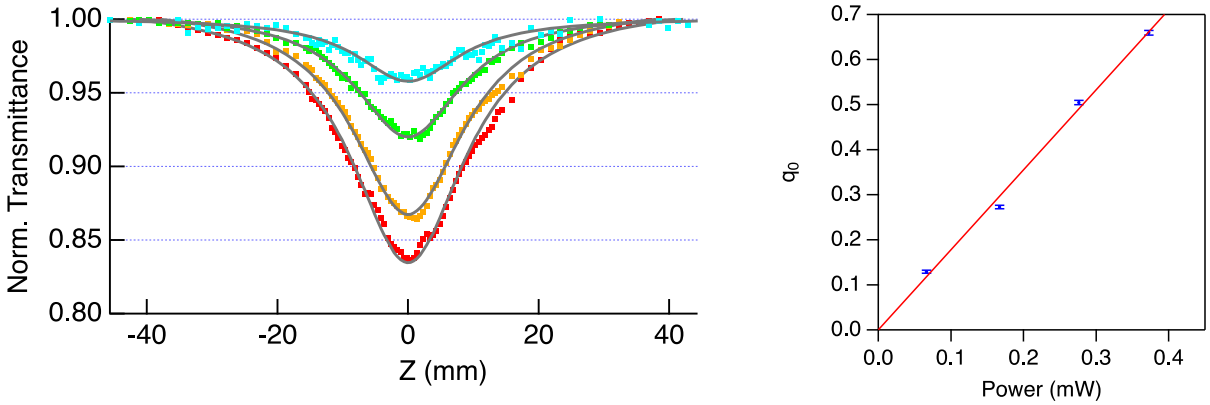

Figure S4. Open aperture Z-scan traces (dots) of **P4** in dichloromethane (2.1 mM, pathlength = 2 mm) at various incident powers (0.07–0.37 mW) at 639 nm with the theoretical fitting curves (solid line) with TPA for temporal and spatial Gaussian pulses (left) and the plot of the obtained on-axis peak two-photon absorbance q_0 with error bars ($\pm\sigma$) against the incident powers with a liner fit (right).

NMR spectra of the new compounds

1,6,7,12-Tetrakis[4-(4-(5-ethynylthiophen-2-yl)-7-(thiophen-2-yl)benzo[c][1,2,5]thiadiazole)phenoxy-N,N'-(2,6-diisopropylphenyl)perylenetetracarboxy-3,4:9,10-diimide (P2)

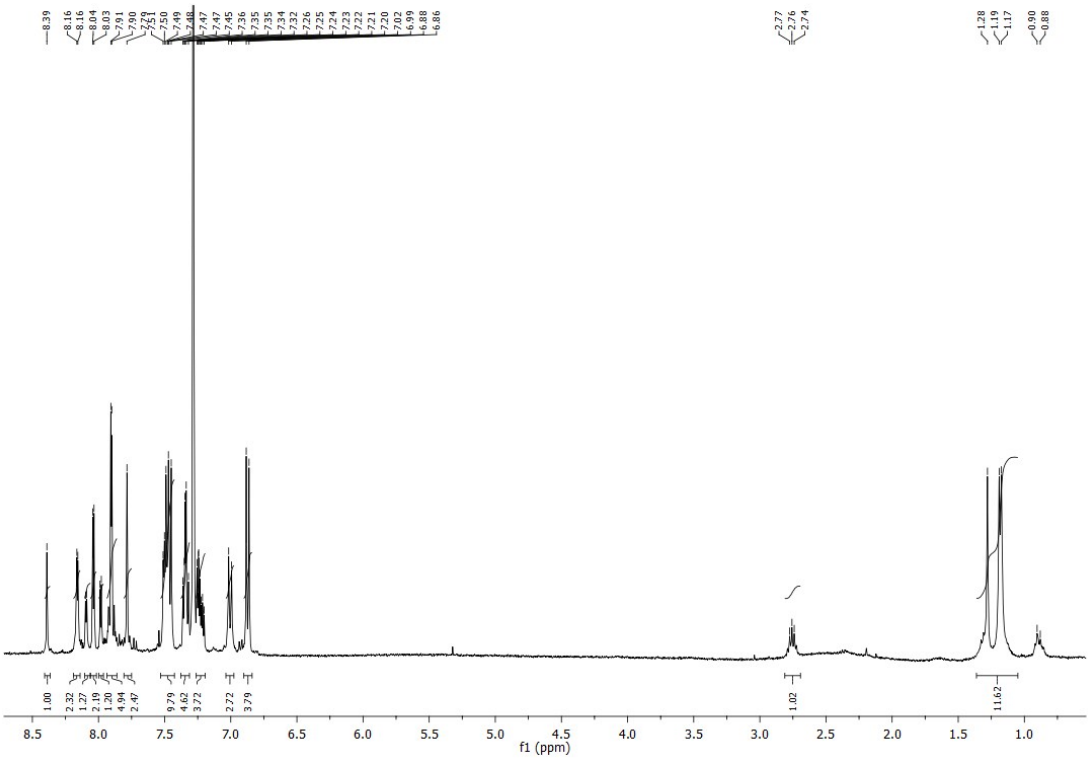

Figure S5. ^{1}H-NMR (400 MHz; $CDCl_3$)

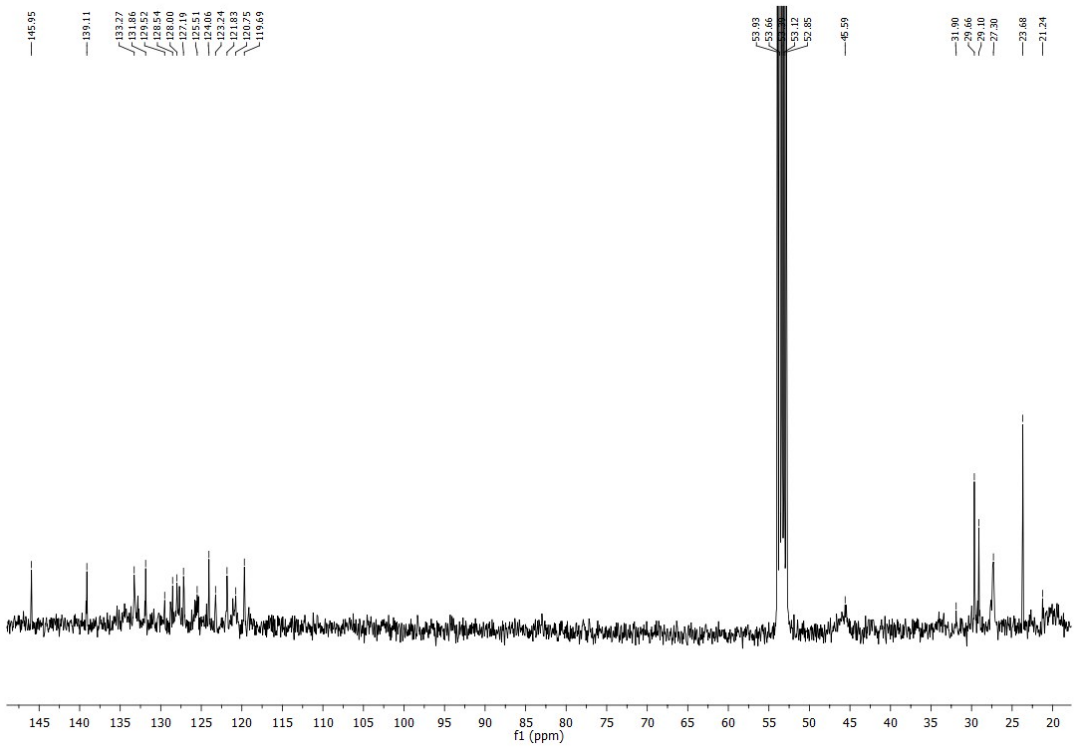

Figure S6. ^{13}C-NMR (100 MHz; CD_2Cl_2)

1,6,7,12-Tetrakis[4-(pyrenethynyl)phenoxy-N,N'-(2,6-diisopropylphenyl)perylenetetracarboxy-3,4:9,10-diimide (P3)

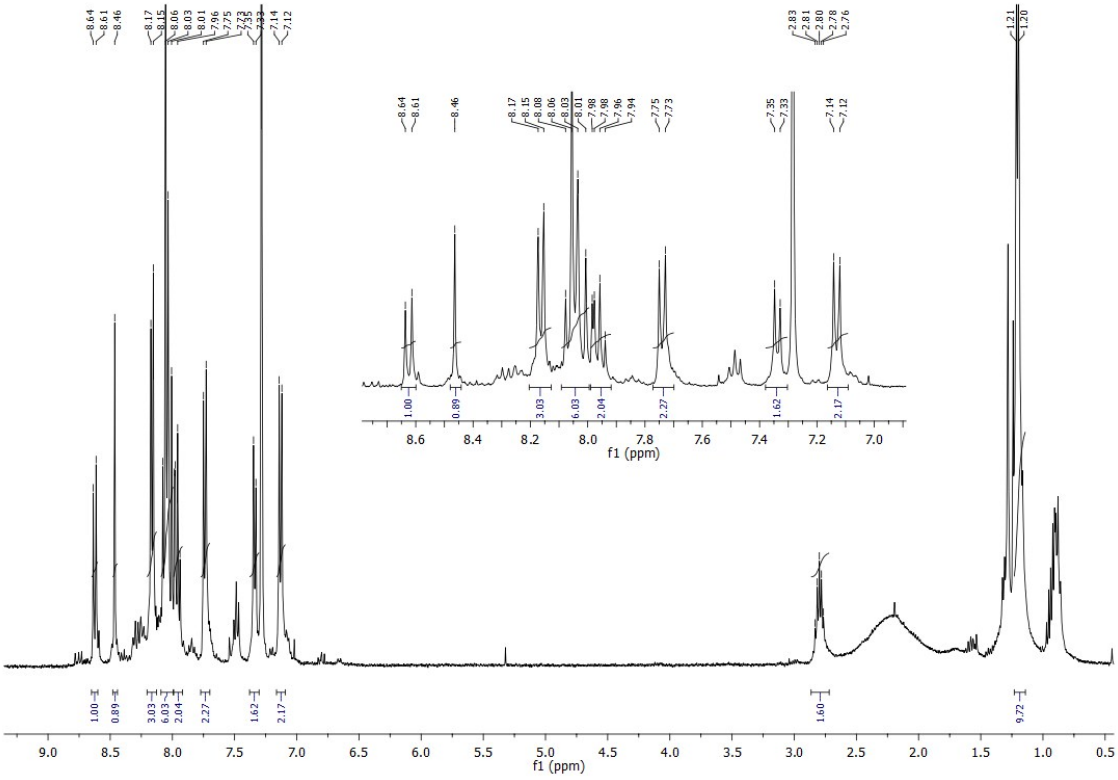

Figure S7. ^{1}H-NMR (400 MHz; $CDCl_3$)

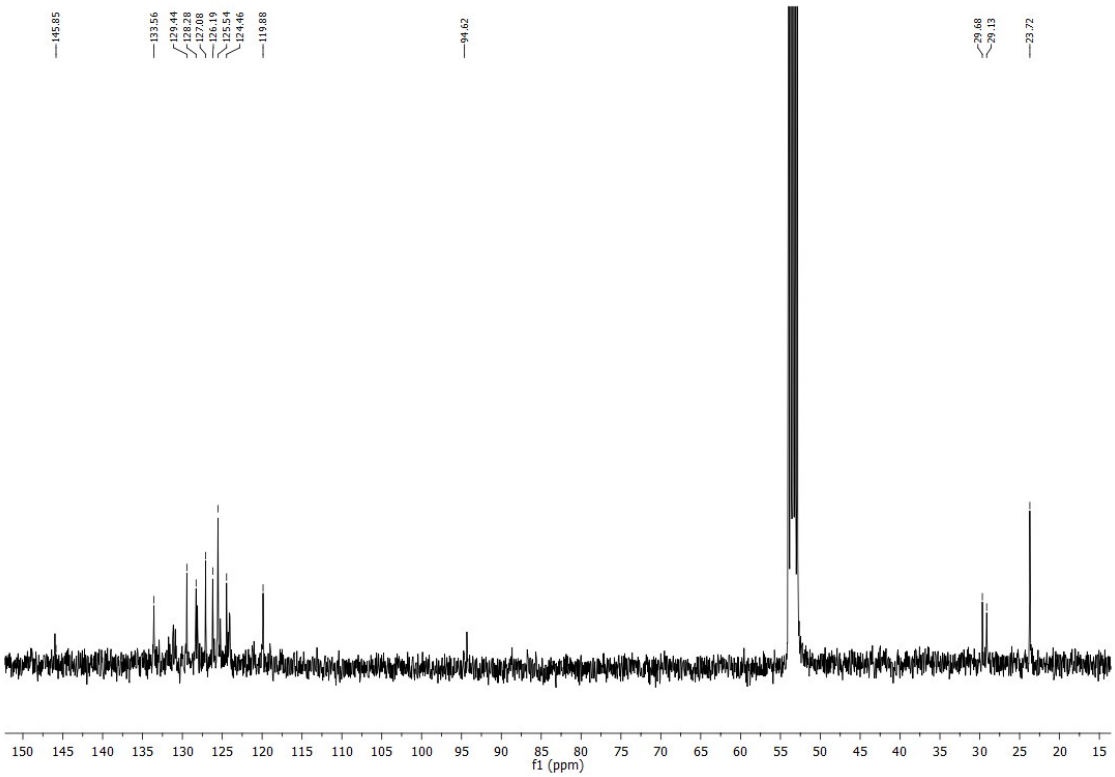

Figure S8. ^{13}C-NMR (100 MHz; CD_2Cl_2)

1,6,7,12-Tetrakis[4-(1-((2-propynyloxy)methyl)pyrene)phenoxy-N,N'-(2,6-diisopropylphenyl)perylenetetracarboxy-3,4:9,10-diimide (P4)

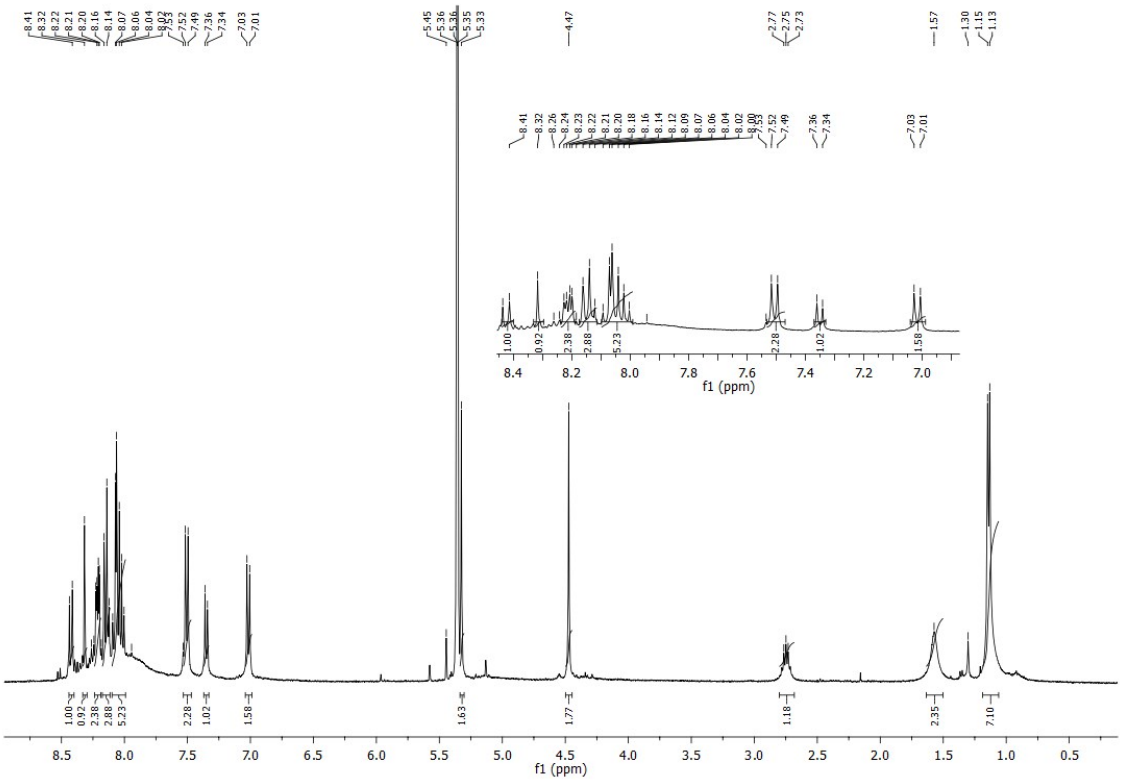

Figure S9. ^{1}H-NMR (400 MHz; CD_2Cl_2)

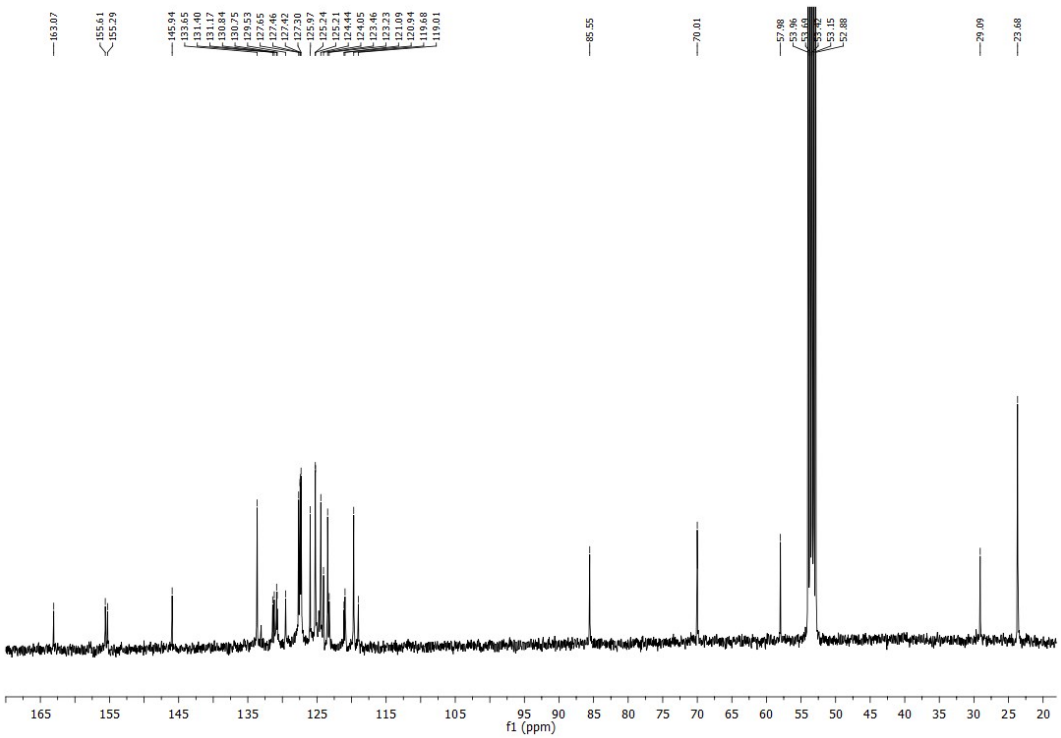

Figure S10. ^{13}C-NMR (100 MHz; CD_2Cl_2)

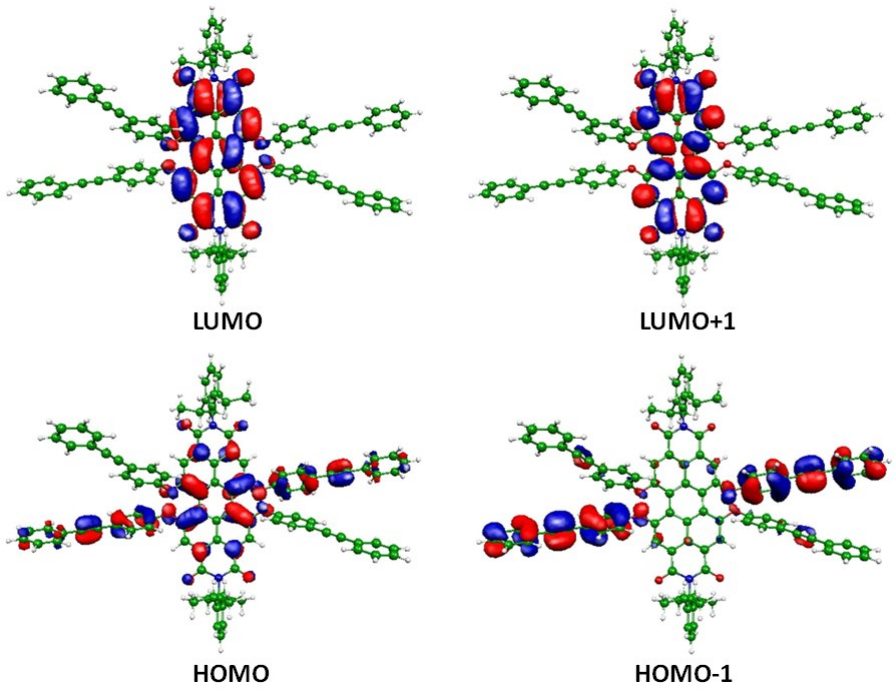

Figure S11. Isodensity plots of the frontier molecular orbitals of **P1** (isodensity contour = 0.02).

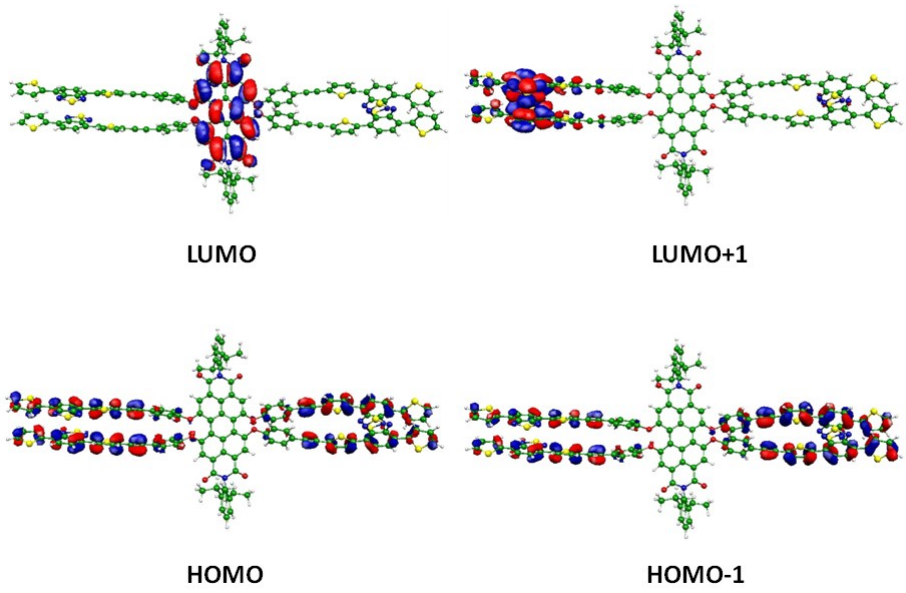

Figure S12. Isodensity plots of the frontier molecular orbitals of **P2** (isodensity contour = 0.02).

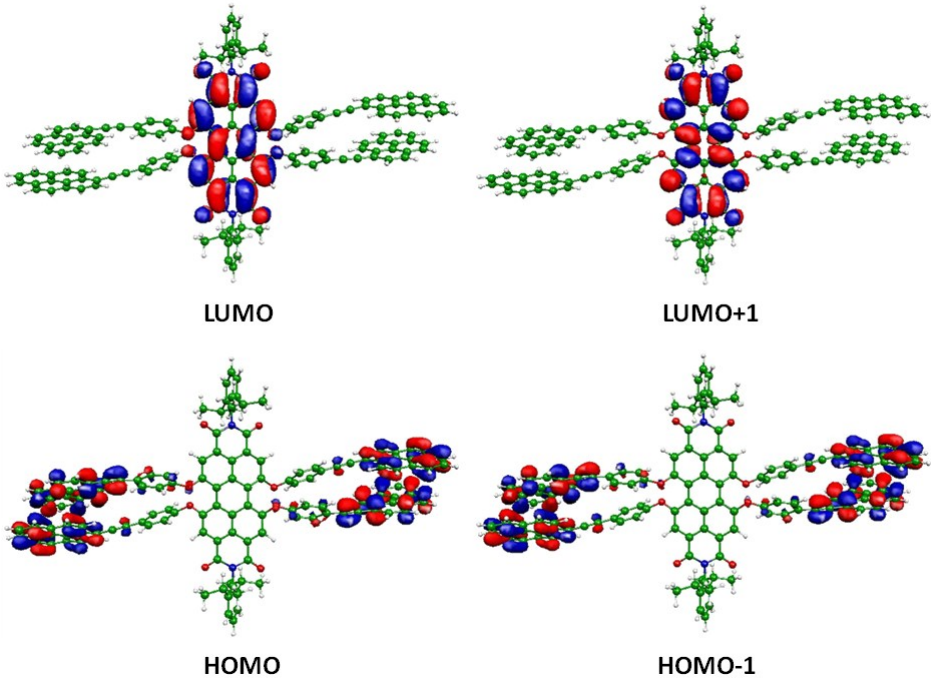

Figure S13. Isodensity plots of the frontier molecular orbitals of **P3** (isodensity contour = 0.02).

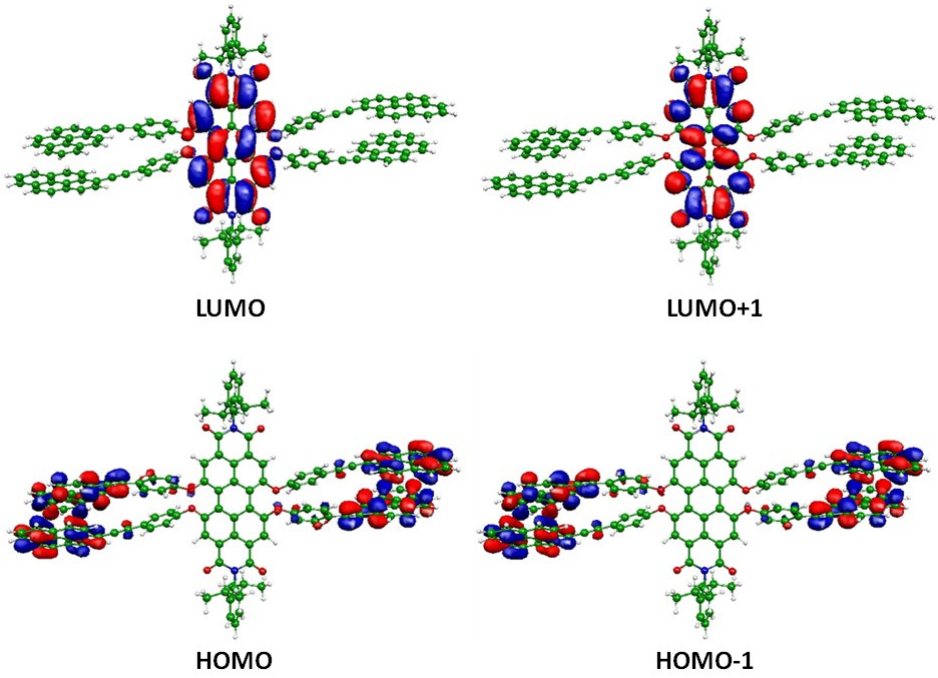

Figure S14. Isodensity plots of the frontier molecular orbitals of **P4** (isodensity contour = 0.02).